

Finite size effects on the electrical properties of sol–gel synthesized  $\text{CoFe}_2\text{O}_4$  powders:  
deviation from Maxwell–Wagner theory and evidence of surface polarization effects

This content has been downloaded from IOPscience. Please scroll down to see the full text.

2007 J. Phys. D: Appl. Phys. 40 1593

(<http://iopscience.iop.org/0022-3727/40/6/001>)

View [the table of contents for this issue](#), or go to the [journal homepage](#) for more

Download details:

IP Address: 14.139.185.18

This content was downloaded on 31/07/2014 at 04:54

Please note that [terms and conditions apply](#).

# Finite size effects on the electrical properties of sol–gel synthesized $\text{CoFe}_2\text{O}_4$ powders: deviation from Maxwell–Wagner theory and evidence of surface polarization effects

Mathew George<sup>1</sup>, Swapna S Nair<sup>1</sup>, K A Malini<sup>1</sup>, P A Joy<sup>2</sup> and M R Anantharaman<sup>1,3</sup>

<sup>1</sup> Department of Physics, Cochin University of Science and Technology, Cochin-682 022, India

<sup>2</sup> Physical Chemistry Division, National Chemical Laboratory, Pune-411 008, India

E-mail: [mra@cusat.ac.in](mailto:mra@cusat.ac.in)

Received 26 August 2006, in final form 4 December 2006

Published 2 March 2007

Online at [stacks.iop.org/JPhysD/40/1593](http://stacks.iop.org/JPhysD/40/1593)

## Abstract

Fine particles of cobalt ferrite were synthesized by the sol–gel method. Subsequent heat treatment at different temperatures yielded cobalt ferrites having different grain sizes. X-ray diffraction studies were carried out to elucidate the structure of all the samples. Dielectric permittivity and ac conductivity of all the samples were evaluated as a function of frequency, temperature and grain size. The variation of permittivity and ac conductivity with frequency reveals that the dispersion is due to Maxwell–Wagner type interfacial polarization in general, with a noted variation from the expected behaviour for the cold synthesized samples. High permittivity and conductivity for small grains were explained on the basis of the correlated barrier-hopping model.

## 1. Introduction

Magnetic nanoparticles continue to be a fascinating subject of interest from both the fundamental and the application points of view [1]. Below a critical size, magnetic particles become single domain in contrast to the multidomain structure of the bulk magnetic materials and these nanomagnetic materials exhibit unique phenomena such as superparamagnetism [2], quantum tunnelling of magnetization [3], etc. Owing to the unique physical properties, magnetic nanoparticles have potential applications in diverse areas such as information storage [4], colour imaging [5], ferrofluids [6] and magnetic refrigeration [7].

Cobalt ferrite ( $\text{CoFe}_2\text{O}_4$ ) is a spinel which possesses a collinear ferrimagnetic structure [8–11]. This spinel was observed to be partially inverse with the formula

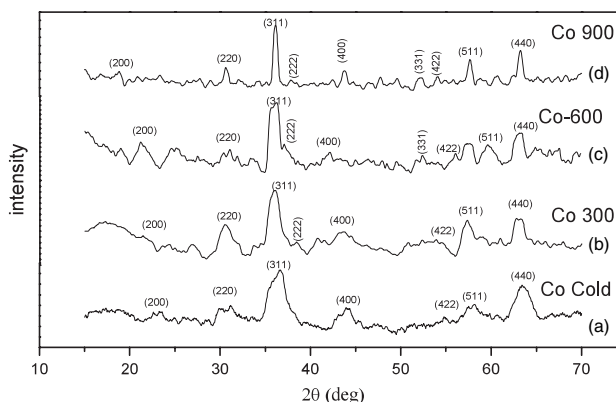
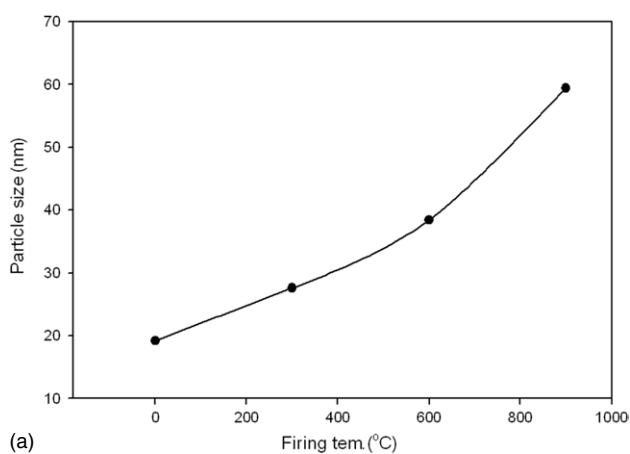


**Figure 1.** XRD pattern of the (a) as prepared  $\text{CoFe}_2\text{O}_4$  powder, (b) the  $\text{CoFe}_2\text{O}_4$  powder heated at 300 °C, (c) at 600 °C and (d) at 900 °C.

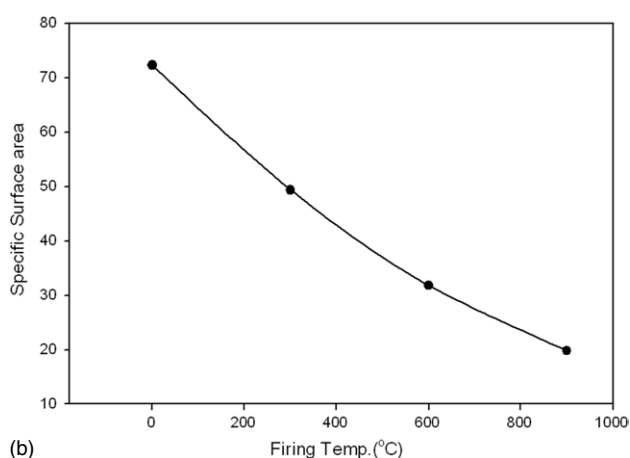
<sup>3</sup> Author to whom any correspondence should be addressed.

**Table 1.** Structural parameters of CoFe<sub>2</sub>O<sub>4</sub> samples.

| Firing temperature (°C) | Particle Size (nm) | Specific surface area (m <sup>2</sup> g <sup>-1</sup> ) | Theoretical density (g cm <sup>-3</sup> ) | Experimental density (g cm <sup>-3</sup> ) | Porosity (%) |
|-------------------------|--------------------|---|---|--|--------------|
| As prepared powder      | 19.2               | 72.3  | 5.19                                      | 4.32                                       | 16.76        |
| 300                     | 27.6               | 49.4  | 5.20                                      | 4.44                                       | 14.6         |
| 600                     | 38.4               | 31.81   | 5.24                                      | 4.91                                       | 6.2          |
| 900                     | 59.4               | 19.8  | 5.28                                      | 5.08                                       | 3.9          |



(a)

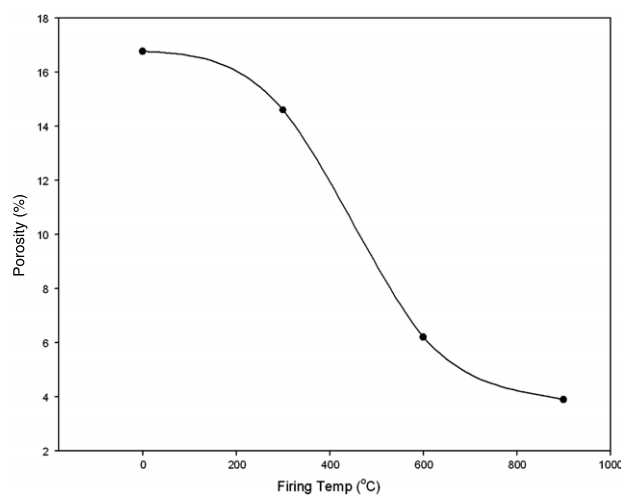


(b)

**Figure 2.** (a) Dependence of particle size. (b) Specific surface area with firing temperature.

(Co<sub>x</sub>Fe<sub>1-x</sub>)[Co<sub>1-x</sub>Fe<sub>1+x</sub>O<sub>4</sub>], where the round and square brackets indicate A and B sites, respectively. The ratio Fe(A)/Fe(B) has been found to vary from  $0.61 \pm 0.04$  to  $0.87 \pm 0.04$  for two extremes [10].

A survey of the literature reveals that detailed studies on the electrical properties of cobalt ferrites have been carried out [12–14]. However, a systematic study on the electrical properties of nanosized cobalt ferrites has seldom been reported. Ferrites, which are very good dielectric materials, have a wide range of applications ranging from microwave frequencies to radio frequencies. The electrical properties of ferrites are dependent upon several factors, namely, the method of preparation, the grain size, the chemical composition, etc [15]. The conduction mechanism in ferrites is quite different from that in semiconductors. In ferrites the temperature dependence of mobility affects the conductivity and the carrier

**Figure 3.** Variation of porosity with firing temperature for the sol-gel synthesized CoFe<sub>2</sub>O<sub>4</sub> powders.

concentration is almost unaffected by temperature variation [16]. Ferrites behave as inhomogeneous dielectric materials in which the individual high conducting grains are separated by low conducting layers [17–19]. The study of the electric properties of ferrites gives valuable information regarding the behaviour of localized electric charge carriers leading to a greater understanding of the mechanism of dielectric polarization of the ferrites.

In the present work, CoFe<sub>2</sub>O<sub>4</sub> has been prepared in the nanoregime with varying particle dimensions. Structural characterization was carried out and grain sizes were estimated using the x-ray diffraction (XRD) technique. The dielectric properties have been evaluated and the effect of the grain size on the dielectric properties has been discussed and the deviation from the theoretical behaviour has been explained by the assumption of surface polarization and porosity. A survey of the literature shows that such a systematic study on the effect of the grain size on the electrical properties of sol-gel derived samples were seldom reported.

## 2. Experimental techniques

### 2.1. Synthesis techniques

Fine particles of CoFe<sub>2</sub>O<sub>4</sub> have been prepared by the sol-gel technique. Analytical grades of Fe(NO<sub>3</sub>)<sub>3</sub> · 9H<sub>2</sub>O and Co(NO<sub>3</sub>)<sub>2</sub> · 6H<sub>2</sub>O were dissolved in ethylene glycol in a 2:1 ratio at about 40 °C. After heating the sol of the metal compounds at around 60 °C a wet gel is obtained. The obtained gel when dried at about 100 °C self-ignites to give a highly voluminous and fluffy product. On heating different portions

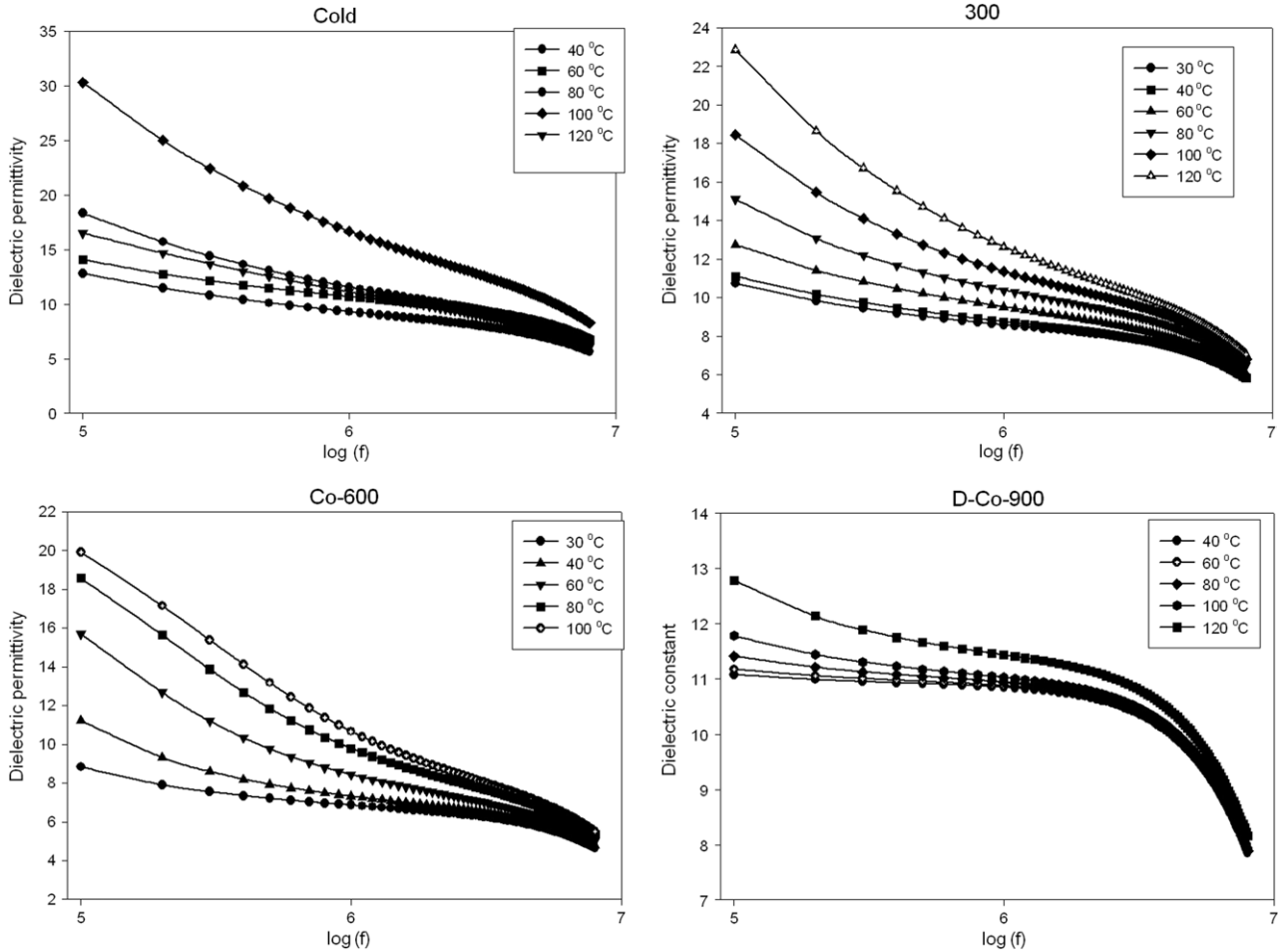


Figure 4. Variation of dielectric permittivity with logarithmic frequency.

of the as prepared powder at 300, 600 and 900 °C for 12 h separately, CoFe<sub>2</sub>O<sub>4</sub> with varying grain sizes were obtained.

## 2.2. XRD studies:

The structural characterization of all the four samples was carried out by the XRD technique on a Rigaku D<sub>max</sub>/2C diffractometer with a nickel filter using Cu-K $\alpha$  radiation (wavelength  $\lambda = 1.5406 \text{ \AA}$ ). The average crystallite size was determined from the measured width of their diffraction maxima by using the Debye–Scherrer formula. The x-ray density, apparent density and porosity of the prepared ceramic samples were calculated.

Assuming all the particles to be spherical, the specific surface area was calculated from the relation

$$S = 6000/d_g \rho, \quad (1)$$

where  $d_g$  is the diameter of the crystallite in nm and  $\rho$  is the density of the particle in  $\text{g cm}^{-3}$ , and the porosity was calculated from the observed and the theoretical density for all the four samples.

## 2.3. Electrical characterization

The electrical properties of cobalt ferrite samples were carried out using a home-made cell and an LCR meter HP 4285A.

Pellet-shaped samples were employed for the evaluation of the electrical properties. The dielectric permittivity ( $\epsilon_r$ ) of the samples were calculated using the relation

$$\epsilon_r = \frac{Cd}{\epsilon_0 A}, \quad (2)$$

where  $C$  is the measured value of the capacitance of the sample,  $d$  is the thickness,  $A$  is the surface area and  $\epsilon_0$  is the dielectric permittivity of air. From the dielectric loss and dielectric permittivity, the ac conductivity of ferrite samples can be evaluated using the relation

$$\sigma_{ac} = 2\pi \epsilon_0 \epsilon_r f \tan \delta, \quad (3)$$

where  $f$  is the frequency of the applied field,  $\epsilon_0$  is the absolute permittivity of air,  $\epsilon_r$  is the relative permittivity of the samples and  $\tan \delta$  is the loss factor.  $\sigma_{ac}$  is temperature- and frequency-dependent [15], and it is attributed to the dielectric relaxation caused by localized electric charge carriers which obeys the power law,

$$\sigma_{ac}(\omega, T) = B\omega^n, \quad (4)$$

where  $B$  and  $n$  are composition- and temperature-dependent parameters.

**2.3.1. Structural studies.** Figure 1 shows the XRD pattern of the four samples of CoFe<sub>2</sub>O<sub>4</sub> powders synthesized by the sol–gel technique.

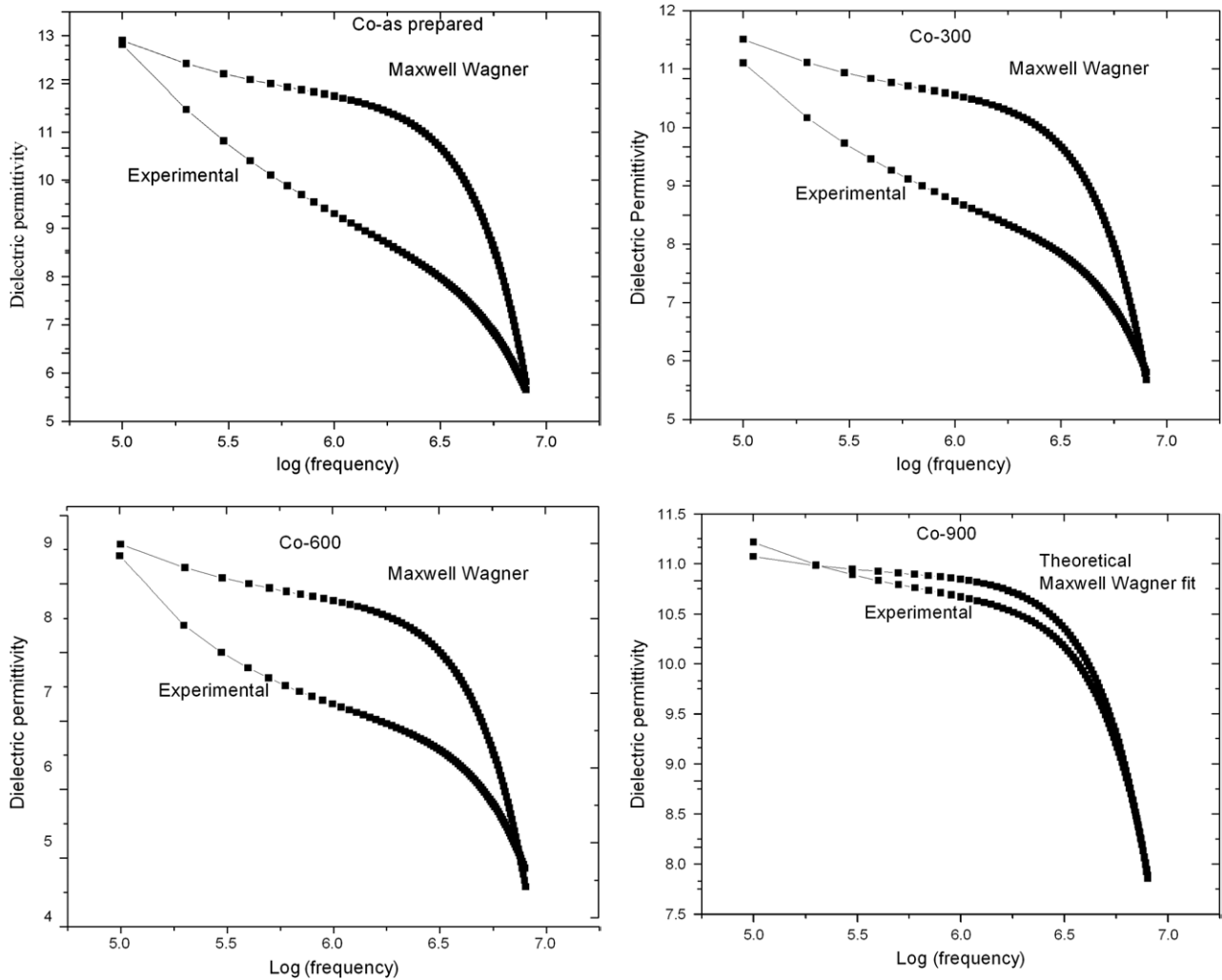


**Figure 5.** Fit to Maxwell–Wagner theory for cobalt ferrite samples synthesized by the sol–gel technique.

The XRD pattern of the samples depicted in figure 1 can be ascribed to spinel  $\text{CoFe}_2\text{O}_4$ . A sharp increase in the crystalline nature of the cobalt ferrite powders was observed as the firing temperature was increased, which is recorded as a decrease in the broadening of the peaks in the diffraction pattern. This clearly shows that the grain size has been increased with an increase in the firing temperature. The grain size of the four samples, heated at different temperatures, was evaluated by employing the Debye–Scherer formula and as shown in table 1.

Figure 2 (a) shows the variation of particle size with the firing temperature for all the four samples.

From the figure it is clear that the grain size increases with the increase in firing temperature. From figure 2(b), it is revealed that the specific surface area of the particle decreases with the increase in firing temperature of the samples, indicating the increase in the grain sizes. However, the specific surface area measurements can have errors in accordance with the error in the determination of the particle size.

Figure 3 represents the variation of the porosity of the samples with the firing temperature.

The porosity decreases with the increase in firing temperature. The study of the porosity and theoretical density becomes important for probing into the dielectric permittivity

of samples. The as prepared samples show very high porosity. The sample fired at  $900^\circ\text{C}$  possesses more than 96% of the theoretical density.

### 2.3.2. Electrical properties.

*Dependence of electrical properties on frequency.* Figure 4 shows the variation of dielectric permittivity with frequency in the range 100 KHz–8 MHz.

Dielectric properties in ferrites are studied well in the bulk level and the permittivity variation can be fitted to the Maxwell–Wagner type of interfacial polarization in many cases. In this model, materials are assumed to be composed of conducting grains separated by poorly conducting grain boundaries. However, in an ultra-fine particle regime, both grains and grain boundaries are larger in number as compared with the bulk case which make the phenomena a little more complex.

Also in nanomaterials, there is an additional chance of getting a high dielectric constant because of large surface polarization owing to the large surface area of individual grains.

In order to probe into the variation pattern of dielectric constant with frequency the experimental data were fitted for

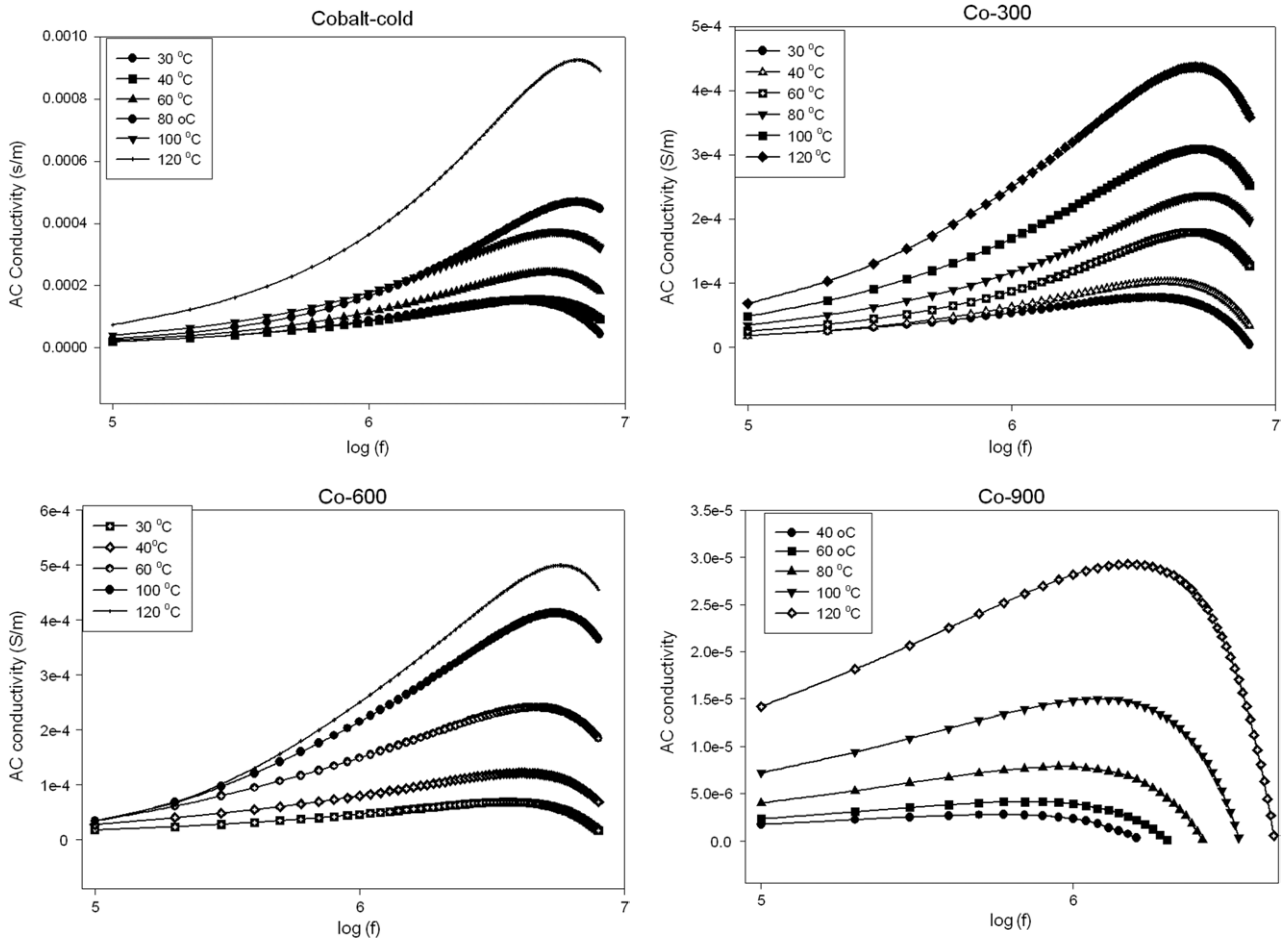


**Figure 6.** Variation of ac conductivity with logarithmic frequency.

the Maxwell–Wagner type interfacial polarization dispersion [18] in agreement with Koops’ phenomenological theory of dielectric dispersion [19]. The theoretical fit gives excellent agreement for the cobalt ferrite samples sintered in 900 °C showing the Maxwell–Wagner type dispersion in the sintered samples (figure 5).

However, in as prepared as well as in the samples sintered at lower temperatures, deviation from Maxwell–Wagner theory is observed, which is evidenced from figure 5. In a low frequency regime, dipolar/interfacial/surface polarization plays a dominant role (than ionic or electronic polarization) in determining the dielectric properties of ferrite materials. In as prepared samples, there is a finite contribution from surface polarization, which gives an initial high value that decays rapidly with frequency as it cannot follow the higher applied frequency. This special observation is evidenced from the high permittivity values for the as prepared samples which fall promptly with frequency for the as prepared samples.

However, in samples sintered at 900 °C, the permittivity variation obeys the Maxwell–Wagner type and the relaxation frequency for the samples is found to be 2.2205 ns for the sample sintered at 900 °C, which increases with the decrease in the grain size.

The frequency dispersion relation given by Habery and coworkers [20, 21] in which the dielectric permittivity

decreases with increasing frequency reaches a constant value for all the samples. Similar behaviour was observed earlier for other systems of ferrites.

The variation of ac conductivity with frequency is shown in figure 6.

The conductivity values at no applied frequencies have been estimated from the graph and plotted in figure 7.

Also the slope of the graphs gives values of  $n$  which determines the conducting behaviour of grains (figure 8(a)):

$$(\sigma_{ac}(\omega, T) = B\omega^n),$$

$$\text{Log}(\sigma_{ac}) = \text{log}B + n\text{log}(\omega).$$

Hence, the slope of  $\text{Log}(\sigma_{ac})$  versus  $\text{log}(\omega)$  graph provides the value of  $n$  while the intercept gives the value of extrapolated conductivity expected at zero applied frequency.

The zero frequency value of conductivity shows an increasing trend with the increase in sintering temperature, while the slope  $n$  decreases with the increase in sintering temperature. This is purely a grain size effect of electrical properties. Hence, the explanation of the typical phenomenon is dealt with in detail in the section ‘Dependence of electrical properties on grain size’.

The conduction is due to the exchange between  $\text{Fe}^{2+} \leftrightarrow \text{Fe}^{3+}$  and due to this exchange displacement of electrons is produced in the direction of the applied field.

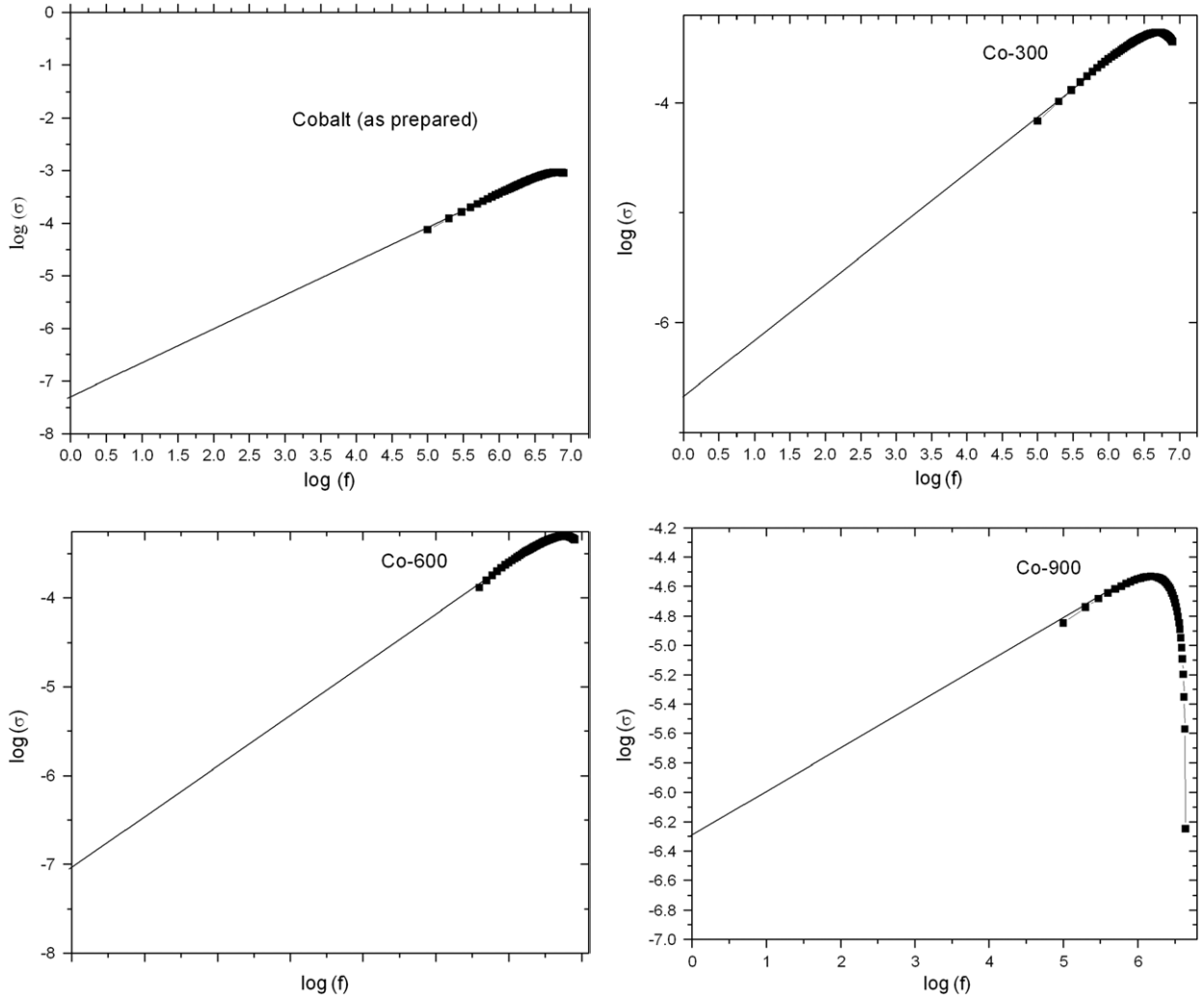


Figure 7. Fit to Koop's theory for the determination of  $\sigma_{dc}$  and  $n$ .

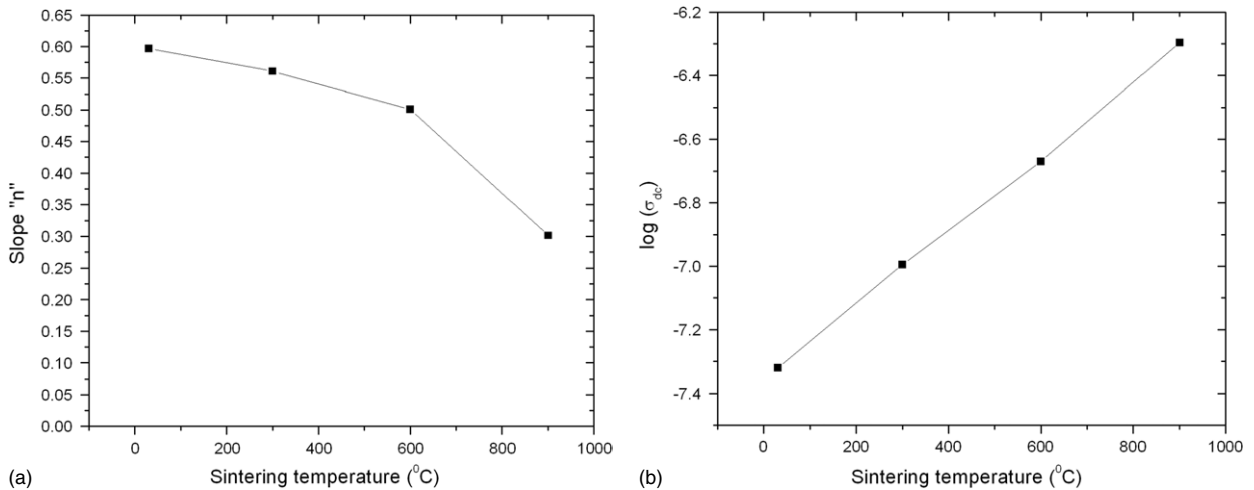
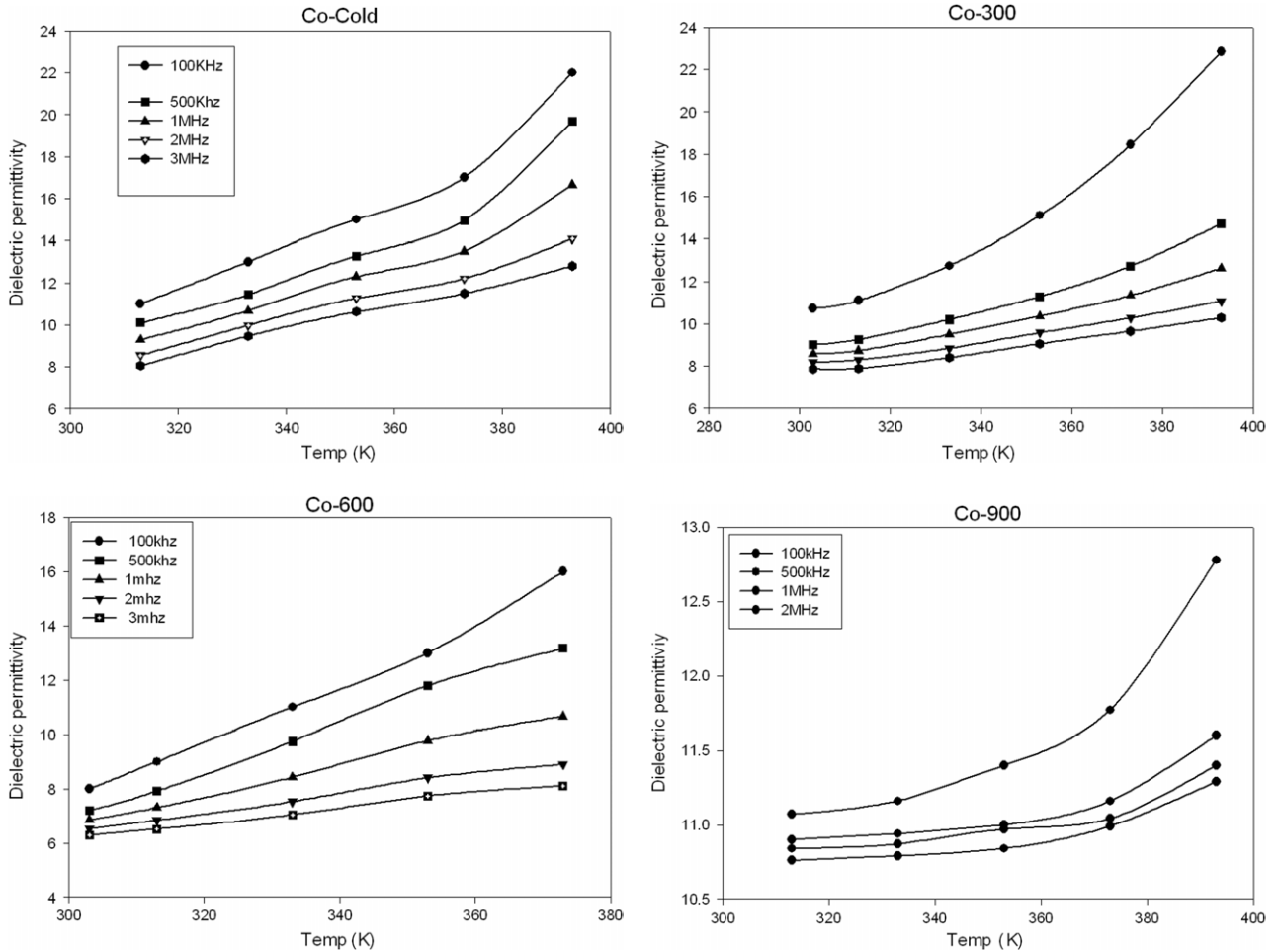


Figure 8. (a) Variation of  $n$  with sintering temperatures. (b) Variation of  $(\sigma_{dc})$  with sintering temperatures.

These electrons determine the polarization in ferrites. The polarization decreases with the increase in frequency and then reaches a constant value due to the fact that, beyond a certain frequency of the external field, the electronic exchange

$Fe^{2+} \leftrightarrow Fe^{3+}$  cannot follow the alternating field. The ac conductivity shows an increasing trend with the increase in frequency for all samples. But at high frequencies the ac conductivity values are less temperature-dependent (figure 6).



**Figure 9.** Temperature dependence of dielectric permittivity.

The variation could be attributed to the Maxwell–Wagner type interfacial polarization model [18, 19].

As the frequency of the applied field increases the conductive grains become more active by promoting the hopping between the  $\text{Fe}^{2+}$  and the  $\text{Fe}^{3+}$  ions on the octahedral sites, thereby increasing the hopping conduction. Thus, we observe a gradual increase in conductivity with frequency. But at higher frequencies the frequency of the hopping ions does not follow the applied field frequency and it lags behind it. This causes a dip in conductivity at higher frequencies.

The relaxation frequencies in ac conductivity is observed to decrease with increasing sintering temperature. The higher relaxation frequencies observed for as prepared as well as low temperature sintered samples are due to smaller grains and higher grain boundaries present in them.

Jonker [17] studied the electrical conduction of a series of ferrites  $\text{Co}_{1-x}\text{Fe}_{2+x}\text{O}_4$  and observed two regions of conductivity. One region was of low conductivity containing  $\text{Co}^{2+}$  and  $\text{Co}^{3+}$  ions and the other type was of high conductivity containing  $\text{Fe}^{2+}$  and  $\text{Fe}^{3+}$  ions. The presence of cobalt on the octahedral site of the spinel favours a conduction mechanism  $\text{Co}^{2+} + \text{Fe}^{3+} \leftrightarrow \text{Co}^{3+} + \text{Fe}^{2+}$ , which explains the predominant conduction mechanism in cobalt ferrite. The presence of impurities can also influence the conductivity of the ferrite [22]. Parker and Elwell studied the electrical conductivity of

$\text{NiFe}_2\text{O}_4$  with a small Co substitution and confirmed the idea of cobalt existing in the ferrite in two valance states [23].

Conductivity change with frequency can be explained using Koop's dispersion relations.

*Dependence of electrical properties on temperature.* Figure 9 shows the variation of dielectric permittivity with temperature.

From these figures it can be seen that the dielectric permittivity increases slowly with temperature in the beginning up to about 373 K and above this the temperature permittivity increases rapidly for all samples. The high dielectric permittivity values at low frequencies found at high temperature may be explained as being due to the presence of permanent dipole moments indicating a small effective charge separation. Such a small separation must be due to asymmetry in the fields experienced by either oxygen or metallic ions. The temperature dependence of permittivity is due to the polarization effect.

The number of space-charge carriers governs the space-charge polarization. As the temperature increases, the number of carriers increases, resulting in an enhanced build-up of space-charge polarization and hence an increase in dielectric properties [23]. It is found that the conductivity saturates at high frequencies. This means that saturation in the



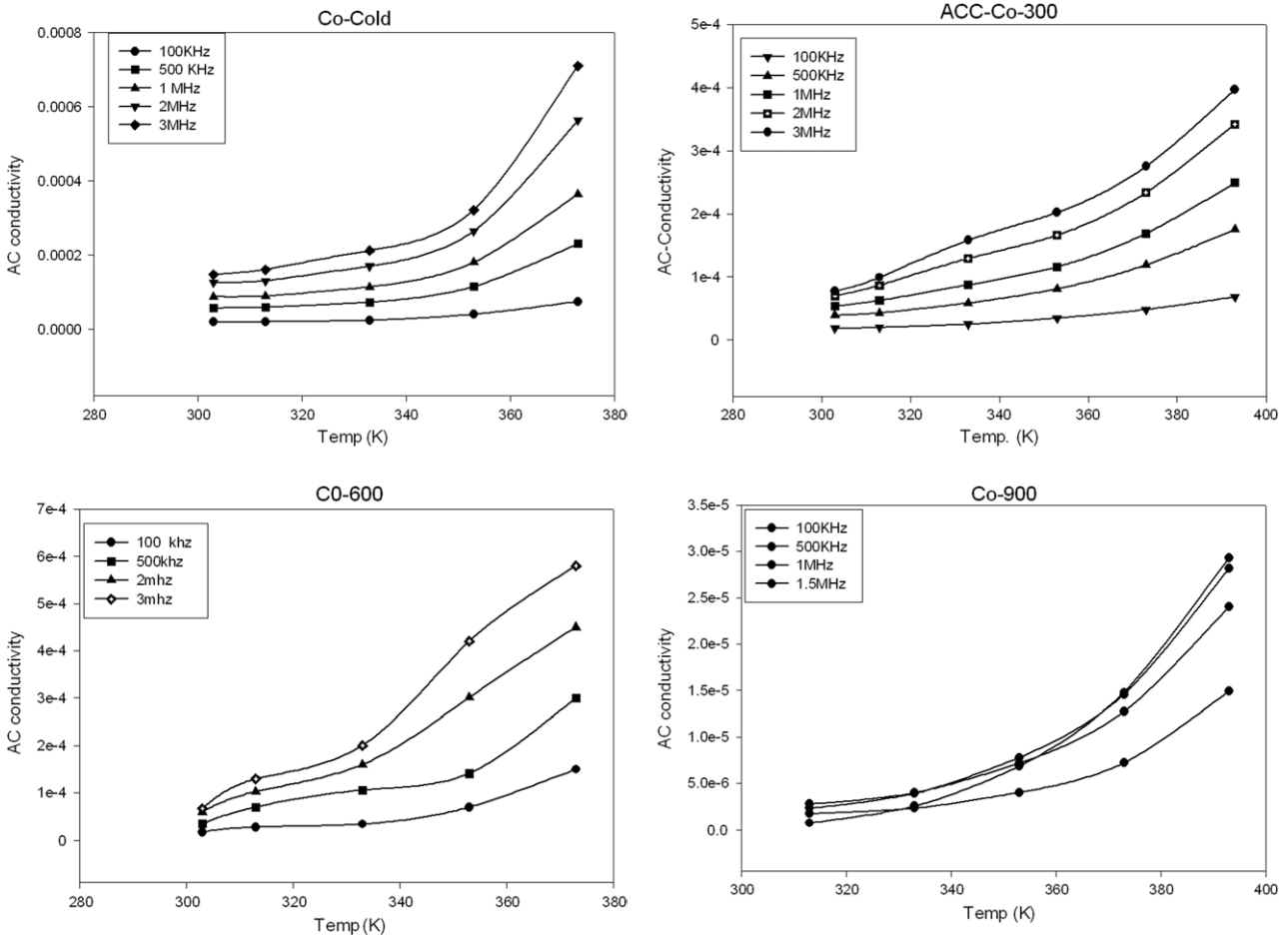


**Figure 10.** Temperature dependence of ac conductivity.

generation of charge carriers was reached at high temperature and high frequency. Therefore, the electronic exchange cannot follow the field variation and hence the dielectric permittivity decreases accordingly. When the temperature increases, the orientation of these dipoles is facilitated and this increases the dielectric polarization. But at very high temperatures the chaotic thermal oscillations of molecules are intensified and the degree of orderliness of their orientation is diminished and thus the permittivity passes through a maximum value.

A similar treatment could be employed for the explanation of the observed conductivity variation (figure 10).

*Dependence of electrical properties on grain size.* The grain size, grain boundaries, porosity, crystal defects and stoichiometry are important factors influencing the conductivity and permittivity. It has been reported [24, 25] that the resistivity of a polycrystalline material in general increases with decreasing grain size. Smaller grains imply a larger number of insulating grain boundaries which act as a barrier to the flow of electrons. Smaller grains also imply smaller grain–grain surface contact area and therefore a reduced electron flow. As expected, the grain size increases with the increase in temperature. Based on the above arguments the resistivity of the ferrites is expected to decrease with the increase in sintering temperature or the increase

in grain size. However, a reverse trend is observed in the present work for sintering the samples up to 900 °C (figure 11).

The comparatively lower value of resistivity or higher value of permittivity in samples sintered at lower temperatures is possibly due to the presence of a localized stage in the forbidden energy gap which arises due to lattice imperfections. The presence of these states effectively lowers the energy barriers to the flow of electrons. At smaller grain sizes, there are twin contributions to the polarization from the larger surface (surface polarization as well as grain boundary contribution), thereby increasing the permittivity values. It is to be noted that in low temperature sintered samples, a higher porosity is observed, which indicates the presence of more number of grain boundaries and this dielectric dispersion can be fitted more to the Onsager three layer spherical capacitor model for dielectric dispersion in multilayers.

According to the correlated barrier-hopping model [16] the ac conductivity may be written as

$$\sigma(\omega) = \frac{\pi^3}{24} N^2 \varepsilon R_\omega^6 \omega, \quad (5)$$

where  $N$  is the concentration of defect sites contributing to the hopping mechanism,  $\varepsilon$  the dielectric permittivity and  $R_\omega$  the

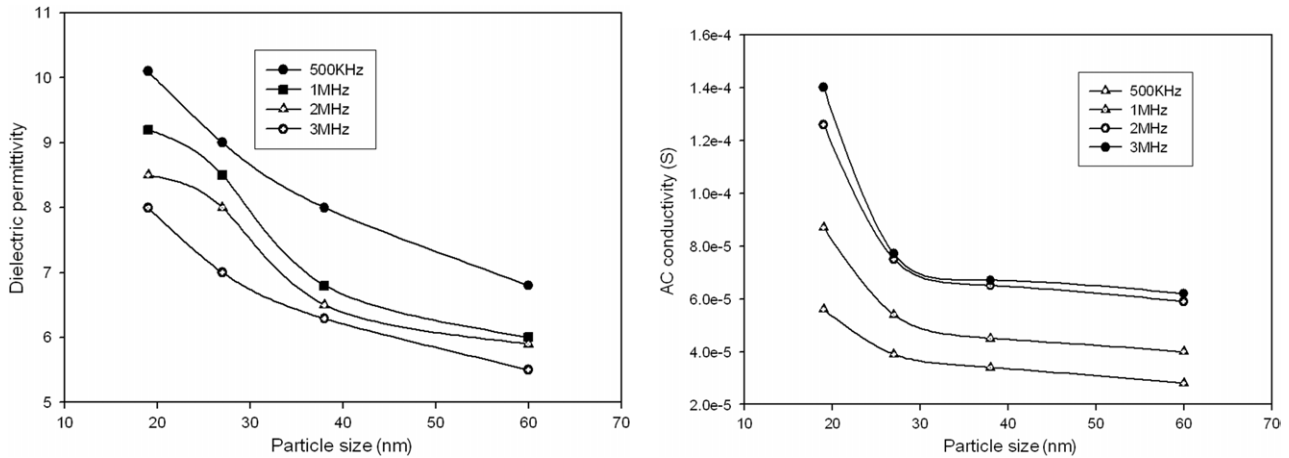


**Figure 11.** Grain size dependence of dielectric permittivity and ac conductivity.

hopping distance. (Here it is to be mentioned that the hopping distance is not a function of the grain size of the sample in general.)

An increase in the sintering temperature increases the grain size as well as the structural refinement as evidenced by the XRD spectra. The results obtained from the structural characterization confirm the increase in crystallinity as well as theoretical density with the increase in grain size/sintering temperature. Hence, sintered samples possess fewer defects as compared with the as prepared or low temperature sintered samples, thus decreasing the value of  $N$  in equation (5), which ultimately reduces the value of ac conductivity. Hence, samples fired at high temperatures or samples with larger grain size exhibit a low value of conductivity. The above discussion suggests that the effect of structure has a greater influence, which is more significant than that of the anticipated effect of grain size. Since the dielectric permittivity is directly proportional to the square root of conductivity, the variation of permittivity with the grain size shows a similar trend.

Also from the graphs in figures 8(a) and (b), it can be concluded that the fast decay (as evidenced from the high value of  $n$  in Koops' equation for conductivity ( $\sigma_{ac}(\omega, T) = B\omega^n$ )) shows that surface effects and crystal defects are present in as prepared as well as in the low temperature sintered samples. They are responsible for the higher value of conductivity, while the extrapolated dc value of conductivity decreases with the decrease in grain size as predicted by the theory.

### 3. Conclusion

Nanoparticles of cobalt ferrite were prepared by a novel sol-gel method in which the as prepared samples themselves are more crystalline than those obtained from the usual chemical co-precipitation techniques. The dependence of both dielectric permittivity and ac conductivity on frequency is in good agreement with Koops' phenomenological theory of dielectric dispersion. A theoretical fit to Koops' dispersion equation is provided and the variation of the power of applied frequency with temperature on the ac conductivity is studied. The high dielectric permittivity at high temperature was

explained as being due to the presence of permanent dipole moments, indicating a small effective charge separation. The enhancement of electric properties with decreasing crystallite size was explained on the basis of the correlated barrier-hopping model. A clear deviation from the Maxwell type of interfacial polarization is observed in as prepared samples because of twin contributions from surface polarization as well as porosity. Conductivity values show a decreasing trend with the increase in grain size, against expectations, which is due to the localized lattice defects present in as prepared as in well as in low temperature sintered samples.

### References

- [1] Dorman J L and Fiorani D 1992 *Magnetic Properties of Fine Particles* (Amsterdam: North Holland)
- [2] Kittel C 1946 *Phys. Rev.* **70** 965
- [3] Chundnovsky E M and Gunther L 1988 *Phys. Rev. Lett.* **60** 661
- [4] Gunther L 1990 *Phys. World* **12** 28
- [5] Ziolo R F 1984 *US Patent* **4** 474866
- [6] Rosenweig R E 1985 *Ferrohydrodynamics* (Cambridge, MA: MIT Press)
- [7] Bautista M C, Bomati-Miguel O, Zhao X, Morales M P, González-Carre T, Pérez de Alejo R, Ruiz-Cabello J and Veintemillas-Verdaguer S 2004 *Nanotechnology* **15** S154
- [8] Lin D, Nunes A C, Majkrzak C F and Berkowitz A E 1995 *J. Magn. Magn. Mater.* **145** 343
- [9] Haneda K and Morrish A H 1988 *J. Appl. Phys.* **63** 3874
- [10] Sawatzky G A, vander Woude F and Morrish A H 1968 *J. Appl. Phys.* **39** 1204
- [11] Cullity B D 1972 *Introduction to Magnetic Materials* (Reading, MA: Addison-Wesley)
- [12] Broemme A D D 1991 *IEEE Trans. Elect. Insul.* **26** 49
- [13] Constantin C and Rosenberg M 1971 *Solid State Commun.* **9** 675
- [14] Griffiths B A, Elwell D and Parker R 1970 *Phil. Mag.* **22** 163
- [15] Reddy P V, Sathyanarayana R and Rao T S 1983 *Phys. Status Solidi.* **78** 109
- [16] Viswanathan B and Murthy V R K 1990 *Ferrite Materials, Science and Technology* (New Delhi : Narosa Publishing House)
- [17] Jonker G H 1959 *J. Phys. Chem. Solids* **9** 165
- [18] Wagner K W 1973 *Am. Phys.* **40** 317
- [19] Koops C G 1951 *Phys. Rev.* **83** 121

- [20] Haberey F and Wijn H P J 1968 *Phys. Status. Solidi.* **26** 231
- [21] Saxena N, Kunar B K, Zaidi Z H and Srivastava G P 1991 *Phys. Status. Solidi. A* **127** 231
- [22] Josyulu O S and Sobhanadri J 1980 *Phys. Status. Solidi. a* **59** 323
- [23] Parker R and Elewell D 1966 *J. Appl. Phys.* **17** 1269
- [24] Kuczynski G C, Hooton N A and Gibbon C F 1967 *Sintering and Related Phenomenon* (New York : Gordon and Breach) p 65
- [25] Pal M, Brahma P and Chakravorthy D 1994 *J. Phys. Soc. Japan* **63** 3356